J|A|C|S
ARTICLES
Published on Web 03/03/2002

Solution Synthesis of Gadolinium Nanoparticles

Jennifer A. Nelson, Lawrence H. Bennett, and Michael J. Wagner*

Contribution from the The George Washington University, Department of Chemistry, Washington, DC 20052

Received October 1, 2001

Abstract: Gadolinium nanoparticles have been produced at subambient temperature by alkalide reduction. The nanoparticles display maxima in the temperature dependence of their magnetization, cooled in the absence of an applied external field, at T_{max} of 5.0 and 17.5 K for unheated samples and samples annealed at 1000 °C for 4 h, respectively. Field cooled behavior deviates at temperatures slightly above T_{max}, increasing at lower temperature. Curie−Weiss law fits of the high-temperature data yield magnetic moments in close agreement with those expected for noninteracting Gd^{3+} ions, suggesting that the behavior seen is due to a magnetic transition rather than superparamagnetism. Magnetization is linearly dependent on field at temperatures higher than 7−8 times T_{max} and shows remanence-free hysteresis at lower temperature, suggesting metamagnetism. Some annealed samples show evidence of additional ferromagnetic interactions below ~170 K. Magnetic entropy curves generated from magnetization data are consistent with that expected for a paramagnet.

Introduction

Nanoscale lanthanides and their alloys are of current interest due to their magnetic properties and the potential enhancement that nanoscale, nanostructure, or nanocomposite materials may exhibit. Six of the nine elements that display ferromagnetism are lanthanides ($Z = 64-69$). All six have magnetic moments per atom that exceeds that of iron.[1] Compounds and alloys of lanthanides are materials of choice in many applications requiring high-quality hard or soft magnets.[2] Nanoscale magnetic materials are of interest for application as ferrofluids, in high-density magnetic storage, in high-frequency electronics, as high performance permanent magnets, and, of particular interest to our research, as magnetic refrigerants.

Magnetic refrigeration is a potentially highly energy efficient cooling method free of environmentally deleterious working fluids (e.g., chlorofluorocarbons). Rather than compression/expansion cycles characteristic of gas refrigerators, magnetic refrigeration relies on the magnetocaloric effect, the change in temperature associated with the magnetization/demagnetization of a magnetic material. In the low temperature range ($T < 20$ K), the magnetic refrigerants of choice have traditionally been paramagnetic materials, while higher temperatures have utilized ferromagnets. Recently it was suggested and later shown that ferromagnetically interacting superparamagnetic nanomaterials, termed "superferromagnets", can have enhanced ΔT values for either temperature range and may allow operation at lower magnetic fields.[3−7] In addition, magnetic nanomaterials may offer lower losses due to irreversible processes such as eddy currents and hysteresis and better heat transfer.

Utilization of magnetic refrigeration at high temperature depends on the development of materials with sufficiently large change in their magnetic entropy at sufficiently low applied fields. Lanthanide metals, their alloys and compounds exhibit some of the largest high temperature magnetocaloric effects known. Gadolinium is particularly promising, in fact, it is the refrigerant in most magnetic refrigerators operating at room-temperature today.[8] Gadolinium is a ferromagnetic metal with a large moment and whose Curie temperature, 293.2 ± 0.4 K,[2] is close to ambient. Gadolinium, its alloys, and its compounds exhibit the largest magnetocaloric effects known near room temperature.[9]

To date, only two reports of gadolinium nanoparticles, prepared by gas-phase methods in both cases, have appeared. The dependence of the particle size and distribution on preparation parameters was examined[10] and the magnetic properties studied.[11] To our knowledge, there have been no reports of *any* lanthanide nanoparticles, much less gadolinium nanoparticles, synthesized by chemical means. This is unfortunate as solution methods offer the advantages of simplicity, stoichiometric control, ease of scale-up, and the possibilities of

* To whom correpondence should be addressed.

(1) Cullity, B. D. *Introduction to Magnetic Materials*; Addison-Wesley Publishing Company: Reading, MA, 1972.
(2) Jakubovics, J. P. *Magnetism and Magnetic Materials*; University Press: Cambridge, 1994.
(3) Shull, R. D.; Swartzendruber, L. J.; Bennett, L. H. Proceedings of the 6th International Cryocoolers Conference, David Taylor Research Center, Anapolis, MD, 1991; p 231.
(4) McMichael, R. D.; Ritter, J. J.; Shull, R. D. *J. Appl. Phys.* **1993**, *73*, 6946−6948.
(5) McMichael, R. D.; Shull, R. D.; Swartzendruber, L. J.; Bennett, L. H.; Watson, R. E. *J. Magn. Magn. Mater.* **1992**, *111*, 29.
(6) Bennett, L. H.; McMichael, R. D.; Swartzendruber, L. J.; Shull, R. D.; Watson, R. E. *J. Magn. Magn. Mater.* **1992**, *104−107*, 1094.
(7) Bennett, L. H.; McMichael, R. D.; Tang, H. C.; Watson, R. E. *J. Appl. Phys.* **1994**, *75*, 5493.
(8) Bohigas, X.; Molins, E.; Roig, A.; Tegada, J.; Zhang, X. X. *IEEE Trans. Magn.* **2000**, *36*, 538.
(9) Giguere, A.; Foldeaki, M.; Gopal, B. R.; Chahine, R.; Bose, T. K.; Frydman, A.; Barclay, J. A. *Phys. Rev. Lett.* **1999**, *83*, 2262.
(10) Shao, Y. Z.; Shek, C. H.; Lai, J. K. L. *J. Mater. Res.* **1998**, *13*, 2969.
(11) O'Shea, M. J.; Perera, P. *J. Appl. Phys.* **1999**, *85*, 4322.

10.1021/ja0122703 CCC: $22.00

size control with narrow size distributions. However, the synthesis of lanthanide nanoparticles is challenging due to their high reduction potential and their extremely reactive nature as nanoscale materials. So, while there are a number of solution methods for the synthesis of nanoscale materials, including metal evaporation into organic matrixes,[12] sonochemical methods,[13] and reduction of metal salts in solution,[14−20] none have been proven capable of producing lanthanide metal nanoparticles to date.

Alkalides are crystalline ionic salts consisting of crown ether or cryptand complexed alkali metal cations charge balanced by a stoichiometric number of alkali metal anions.[21,22] Alkalides produce alkali metal anions when dissolved in nonreducible solvents. The alkali metal anion is nearly as thermodynamically powerful a reductant as a solvated electron, the most powerful reductant possible in any given solvent, and is capable of simultaneous two electron transfers. Mixing of alkalide and metal salt solutions results in the formation of a colloid of nanoscale (∼2−15 nm diameter) particles with a narrow size distribution. Colloid stability varies from minutes to hours, depending on the metal reduced and the reaction conditions. Following aggregation and removal of the solvent, the byproducts can be washed away, recovering the crown ether and leaving bare metal nanoparticles. Supported as well as bare metal particles can be produced.[23−26]

Previous studies showed the general applicability of the alkalide reduction method to producing nanoparticles of elements from the early transition metals to p-block semimetals. Here we report the extension of this method into the lanthanides. Specifically, we report the synthesis of nanoscale Gd particles by alkalide reduction and their magnetic characterization.

Experimental Section

Nanoscale gadolinium metal was synthesized by homogeneous alkalide reduction according to the following scheme:

$$3\,K^+(15\text{-crown-}5)_2Na^- + 2GdCl_3 \xrightarrow{THF} 2Gd_{nano} + 3K^+(15\text{-crown-}5)_2Cl^- + 3\,NaCl$$

$GdCl_3$ (anhydrous, 99.99%) was purchased from Aldrich and used without further purification. Crown ether (15-crown-5, 98%) was purchased from Alfa-AESAR, further dried, and then purified by vacuum distillation. Tetrahydrofuran (THF, 99.9+% HPLC grade, inhibitor free) was purified by stirring over KNa alloy until a persistent blue solution was obtained. NH_3 (99.99% anhydrous grade, MG Industries) was purified by vacuum distillation from Na metal. All reactant and product manipulation was performed in a N_2 filled drybox (<1 ppm H_2O and O_2) and solvent transfers were accomplished by vacuum techniques (10^{-6} Torr). Following reduction, excess reductant was removed by repeated washing with THF until the wash was clear. Byproducts were removed by washing repeatedly, with intermediate grindings, with liquid NH_3. Completeness of the removal of organics and the need for additional washing was judged by IR spectroscopy. Sample annealing was done in fused-silica tubing flame sealed under vacuum (10^{-6} Torr). Further synthetic details can be found elsewhere.[23−25]

Magnetic characterization was performed with a Quantum Design model MPMS magnetic property measurement system (SQUID magnetometer) with magnetic quench option. Magnetization measurements of field cooled and zero field cooled samples were obtained with increasing temperature. Samples were vacuum-sealed (10^{-6} Torr) in high-field NMR tubes and placed butt to butt with an empty, vacuum-sealed NMR tube in a sample straw to minimize background diamagnetism. Electron micrographs were obtained on a JEM-1200EX transmissions electron microscope (TEM) operation at 80 keV. Samples for TEM were dispersed in MeOH by sonication and deposited on Formvar holey film/carbon coated copper grids. Powder X-ray patterns were obtained with a Scintag XDS-2000 diffractometer (Cu Kα radiation, 1.54 Å) equipped with a liquid N_2 cooled solid-state detector. Diffraction patterns of air-sensitive samples were obtained using a custom-made air-free holder with Be windows. IR spectra were obtained on pellets made in a drybox by mixing 5 mg of sample into KBr with an agate mortar and pestle.

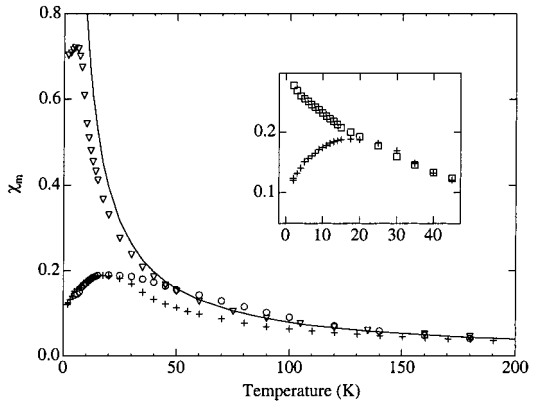

Figure 1. Temperature dependence of the molar magnetic susceptibility (H = 1000 Oe) of Gd nanoparticles unheated (triangles), heated to 1000 °C (crosses), and heated to 1000 °C showing a broadened peak (circles). Solid line is calculated Curie behavior for Gd^{3+}. Inset shows typical deviation of field cooled (squares) from zero field cooled behavior (crosses).

Results

Following synthesis and washing, the gadolinium nanoparticles are in the form of a free-flowing black powder. The nanoparticles are highly pyrophoric, spontaneously igniting immediately, and quite spectacularly, upon exposure to air. Following annealing at 1000 °C for 4 h, the oxidation is far less violent. In either case, the product of exposure is a white powder determined to be cubic Gd_2O_3 by powder XRD. Prior to exposure to air, no crystalline material was observed by powder XRD for either the unheated or the heated samples.

The temperature dependence of the magnetization for samples cooled in zero field (ZFC) is shown in Figure 1. Each sample shows a peak in magnetization, at T_{max} of 5.0 K for unheated samples and 17.5 K for the annealed samples, the later of which we will refer to as Gd(a) samples. In some annealed samples, which we will refer to as Gd(b) samples, the susceptibility decrease above the peak was significantly broadened. In all cases, field-cooled (FC) behavior deviates from ZFC behavior

(12) Klabunde, K. J.; Li, Y. X.; Tan, B. J. *J. Chem. Mater*. **1991**, *3*, 30.
(13) Suslick, K. S.; Hyeon, T.; Fang, M. *Chem. Mater.* **1996**, *8*, 2172.
(14) Kraus, C. A.; Kurtz, H. F. *J. Am. Chem. Soc.* **1925**, *47*, 43.
(15) Schlesinger, H. *J. Am. Chem. Soc.* **1953**, *75*, 215−219.
(16) Rieke, R. D.; Hudnall, P. M. *J. Am. Chem. Soc.* **1972**, *94*, 7178.
(17) Boutonnet, M.; Kizling, J.; Stenius, P.; Maire, G. *Colloids Surf.* **1982**, *5*, 209.
(18) Ritter, J. J. *Adv. Ceram.* **1987**, *21*, 21.
(19) Bonnemann, H.; Brijoux, W.; Joussen, T. *Angew. Chem., Int. Ed. Engl.* **1990**, *29*, 273.
(20) Fievet, F.; Fievet-Vincent, F.; Lagier, J. P.; Dumont, B.; Figlarz, M. *J. Mater. Chem.* **1993**, *3*, 627.
(21) Wagner, M. J.; Dye, J. L. *Annu. Rev. Mater. Sci.* **1993**, *23*, 223.
(22) Wagner, M. J.; Dye, J. L. Alkalides and Electrides. In *Comprehensive Supramolecular Chemistry*; Lehn, J. M., Gokel, G. W., Eds.; Elsevier: Oxford, UK, 1996; Vol. 1, p 477.
(23) Tsai, K.-L.; Dye, J. L. *J. Am. Chem. Soc.* **1991**, *113*, 1650.
(24) Tsai, K. L.; Dye, J. L. *Chem. Mater.* **1993**, *5*, 540.
(25) Dye, J. L.; Tsai, K. L. *Farady Discuss.* **1991**, *92*, 45.
(26) Cowen, J. A.; Tsai, K. L.; Dye, J. L. *J. Appl. Phys.* **1994**, *76*, 6567.

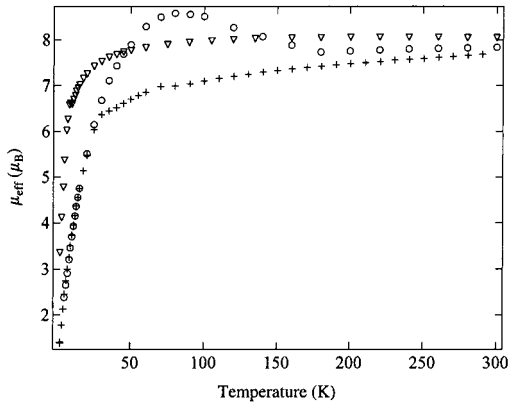

Figure 2. Temperature dependence of the effective moment for Gd nanoparticles unheated (triangles), heated to 1000 °C (crosses), and heated to 1000 °C showing a broadened peak (circles).

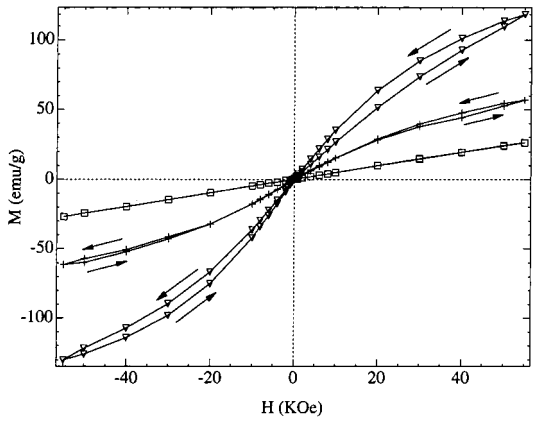

Figure 3. Magnetization loops for unheated (triangles, 5 K; squares, 100 K) and 1000 °C annealed (crosses, 2 K) Gd nanoparticles. Lines between data points are to guide the eye and arrows indicate measurement direction.

at temperatures slightly higher than T_{max}, diverging further at lower temperature (Figure 1, inset). Exposure of the samples to air results in the conversion of the magnetization behavior to the Curie law behavior expected for cubic Gd_2O_3.[27]

The temperature dependence of the magnetization for all samples is fit well as Curie−Weiss law behavior at high temperature. Linear least-squares fits yield values of μ_{eff} of 8.12-(2) μ_B, $\theta = -4.1(4)$ K (40 K < T < 300 K) for unheated samples, 8.06(3) μ_B, $\theta = -31.0(9)$ K (100 K < T < 300 K) for most samples annealed at 1000 °C (i.e., Gd(a) samples), and 8.02(2) μ_B, $\theta = -13.2(6)$ K (200 K < T < 300 K) for Gd(b) samples. Note that the numbers in parentheses are estimates of the standard deviation in the last digit. Also included in Figure 1 for reference is the Curie law temperature dependence of χ_m expected for noninteracting Gd^{3+} ions ($\mu_{eff} = 7.95$ μ_B).[27]

The temperature dependence of μ_{eff} for each sample is shown in Figure 2. Both unheated samples and most of those annealed to 1000 °C show a sharp increase with increasing temperature, leveling off to a steady increase. Gd(b) samples display an initial increase in μ_{eff} that follows closely that seen for Gd(a) samples, deviating at ∼25 K to higher values, peaking at ∼80 K, and then rejoining the behavior of "normal" Gd(a) annealed samples at ∼170 K.

(27) Moon, R. M.; Koehler, W. C. *Phys. Rev.* **1975**, *B11*, 1609.

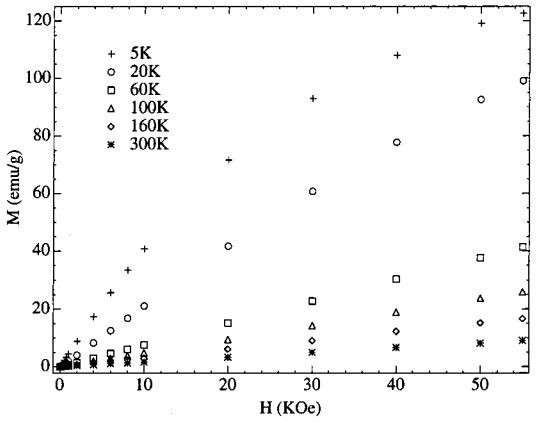

Figure 4. Magnetization curves of unheated Gd nanoparticles at the indicated temperatures. Data presented are decending in field; accending data are excluded for graphical clarity.

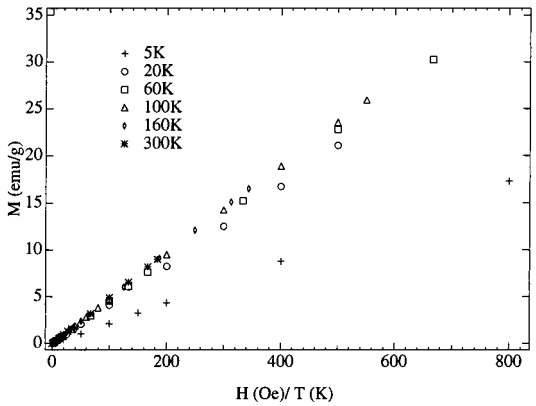

Figure 5. Superimposition of magnetization curves at indicated temperatures.

At temperatures significantly higher than T_{max}, the magnetization is linearly dependent upon field and shows no hysteresis. Marked curvature in the magnetization data is evident at and below T_{max}, with significant remanence-free hysteresis (Figure 3). The loops are not closed, indicating that the anisotropy field is larger than 5.5 T. As the measurement temperature is increased from T_{max}, curvature and hysteresis progressively disappear, becoming negligible above ∼40 and 120 K for unheated and annealed samples, respectively (Figures 4). Plotting the magnetization against H/T shows that the curves superimpose at temperatures above ∼40 and 120 K for unheated and annealed samples, respectively (Figure 5).

The magnetic entropy change ΔS_m, was calculated by numerical integration using the magnetization data and the integrated Maxwell relation[28,29]

$$\Delta S_m(T,H) = \int_0^H \left(\frac{\delta M}{\delta T}\right)_H \mathrm{d}H$$

and is shown in Figure 6. Both unheated and heated samples show steady decreases in ΔS_m with increasing temperature, consistent with that expected for a paramagnet at high temperatures, deviating to slightly lower values as temperature is decreased.

(28) Foldeaki, M.; Chahine, R.; Bose, T. K. *J. Appl. Phys.* **1995**, *77*, 3528.
(29) Foldeaki, M.; Schnelle, W.; Gmelin, E.; Benard, P.; Koszegi, B.; Giguere, A.; Chanine, R.; Bose, T. K. *J. Appl. Phys.* **1997**, *82*, 309.

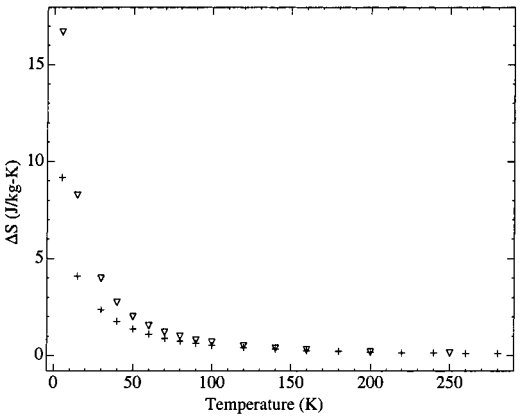

Figure 6. Temperature dependence of the magnetic entropy for unheated (triangles) and 1000 °C annealed (crosses) Gd nanoparticles.

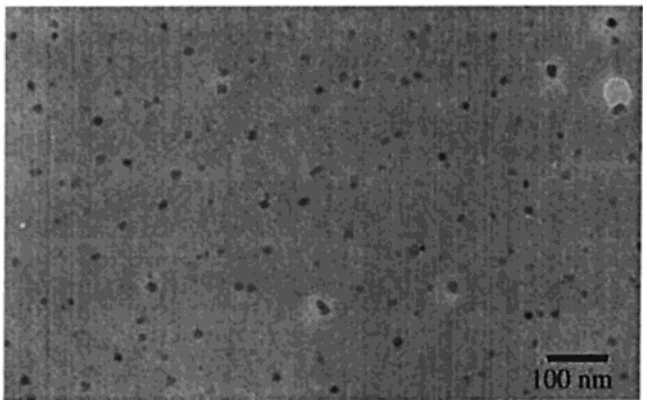

Figure 7. TEM of Gd nanoparticles annealed to 1000 °C. Note that the particles were exposed to air and have been oxidized to Gd_2O_3.

TEM micrographs were obtained for annealed samples. Unfortunately it was necessary to expose the samples to air due to the lack of an air-free insertion system. The samples were slowly oxidized prior to dispersal in MeOH and deposition on grids for analysis. Therefore, the TEM is actually of Gd_2O_3 nanoparticles that are the product of Gd nanoparticle oxidation (Figure 7). Plotting a histogram of the particle diameters measured from the micrographs finds an average particle diameter of 12(3) nm (Figure 8).

Discussion

The temperature dependence of χ_m, both ZFC and FC, found for our Gd nanoparticles is in excellent qualitative agreement with the reported behavior for those produced by multilayer gas-phase deposition.[11] T_{max}s for our unheated and annealed and samples correspond to those previously found for particles of >3 nm and ~ 5 nm, respectively. The later size would seem to conflict with our TEM observations. Assuming that our particles oxidized without interparticle growth, and correcting for the difference in density of Gd and Gd_2O_3, our average diameter for the annealed particles is ~ 11 nm, roughly twice that reported to have approximately the same T_{max}. The violent nature of the oxidation makes the assumption that no particle growth occurred during oxidation somewhat dubious to us. However, while it is clear from TEM micrographs of unheated samples that significant sintering took place even with what we thought to be slowly oxidized sample, the individual particle size ($\sim 1-3$ nm) seems to correspond well with that expected. The annealed sample

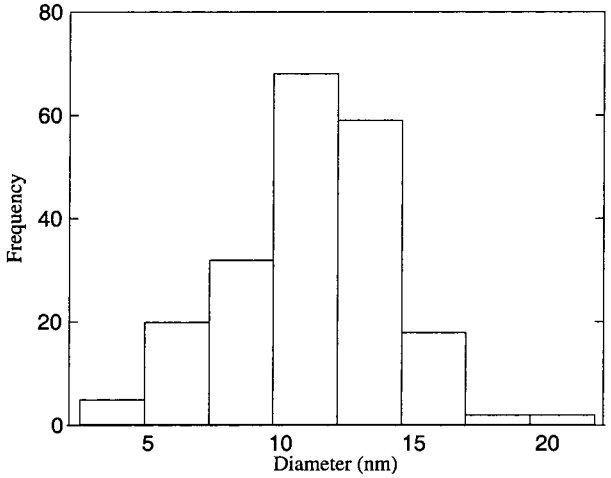

Figure 8. Histogram of the diameters of Gd nanoparticles annealed to 1000 °C (618 particles counted). Note that the particles were exposed to air and are thus oxidized to Gd_2O_3.

oxidizes in a much less violent fashion and the particles seem fairly regular spheroids; multiple particle fusion to create the particles we observe is not evident.

The highly pyrophoric nature of our product, the change in color from black to white, and the production of crystalline Gd_2O_3 upon oxidation are all consistent with behavior expected of Gd nanoparticles. The close agreement of our magnetic data to that reported for Gd nanoparticles prepared by gas phase methods demonstrates that our product is certainly Gd nanoparticles and any oxidation is not severe. Significant oxidation would lead to an additional contribution to the magnetic susceptibility, a "Curie tail". In fact, its manifestation as a contribution proportional to $1/T$, independent of cooling in the presence or absence of a field, would make even a $<1\%$ oxide level distinct. Thus, since no such contribution is observed, it is clear that any oxidation is in fact minimal.

As our particles were produced by a solution method, one might expect that some surface-confined species remain even after copious washing. The byproducts of the reduction, $K^+(15\text{-crown-}5)_2Cl^-$ and NaCl, are both crystalline ionic substances, easily detectable by powder XRD and of good solubility in liquid NH_3. The absence of peaks in the X-ray diffraction pattern is evidence not only that the unheated Gd nanoparticles are either amorphous or of very small size ($<2-3$ nm) but also of the gross removal of the byproducts. More troubling with the alkalide reduction synthesis are decomposition products, as some of these materials are X-ray amorphous organics that have little or no solubility in liquid NH_3. While other solvents may be useful in removing them, it may be better to avoid decomposition altogether. It is important to note that one normally uses an excess of reductant to ensure complete reduction, this excess must not be allowed to thermally decompose on the sample, but must be fully removed in an expeditious manner prior to allowing the sample to warm. This step is critical, a 5% excess of reductant represents a 20% impurity in the product by mass. With careful work, it is possible to avoid decomposition and obtain Gd nanoparticle with no organic impurities detectable by IR spectroscopy, which has been shown to be very sensitive to the presence of decomposition products and can be used to guide the progress of removal of organics.[24]

It should be noted that decomposition products have little effect on the magnetic properties of the Gd nanoparticles, other

than to add a diamagnetic contribution, with a resultant temperature-independent reduction in the gram susceptibility. For magnetic refrigeration, and possibly other applications, it is not at all clear that the presence of surface-confined decomposition products would be disadvantageous. While the added mass would reduce the mass entropy change (i.e., the cooling capacity per unit mass), surface-confined species may present some advantage in protecting the sample from oxidation or providing appropriate spacing between the particles.

The temperature dependence of χ_m is suggestive of magnetically isolated superparamagnetic particles.[30] Further, the superimposition of the hysteresis-free magnetization curves when plotted against *H/T* is consistent with superparamagnetism.[31] However, for a material to be superparamagnetic, the spins within each particle must be strongly coupled so that the particles behave as paramagnets with moments equal to the sum of all of the atomic moments within each particle. The close agreement, within 2%, of the magnetic moments calculated from Curie−Weiss law fitting with that expected for noninteracting Gd^{3+} ions indicates that intraparticle ferromagnetic interactions are insignificant at high temperature. Thus, it seems likely that the high-temperature behavior we observe is simple paramagnetism and the low-temperature behavior is the result of a magnetic phase transition. The interactions responsible for this behavior are evident at temperatures that are 7−8 times T_{max}, judging by the disappearance of hysteresis and deviation from superimposition of *M* vs *H/T* and Curie−Weiss law, indicative of a second-order transition.

The magnetization curves for our Gd nanoparticles show remanence-free hysteresis for temperatures near T_{max}, suggesting metamagnetic behavior similar to that seen for $Gd_5Si_2Ge_2$.[9] No such behavior was reported for Gd nanoparticles produced by gas-phase deposition. In fact, a maximum in the coercivity was reported for particles with diameters ∼10 nm.[11]

Some of our annealed samples showed a broadened peak in the temperature dependence of χ_m. Cooled in the absence of an external field, μ_{eff} closely follows that of the "normal" annealed samples at low temperature. However, as temperature increases, μ_{eff} shows a pronounced rise, breaking with "normal" behavior at ∼25 K and increasing to values larger than expected for a paramagnetic Gd sample, peaking at ∼80 K. This is indicative of additional ferromagnetic interactions below ∼170 K and may be due to some portion of the sample displaying superparamagnetism or superferromagnetism. However, is not clear whether the interactions are inter- or intraparticle, nor is the difference in the preparative method that resulted in this behavior apparent to us.

(30) Dormann, J. L.; Fiorani, D.; Tronc, E. *Adv. Chem. Phys.* **1997**, 283.
(31) Bean, C. P.; Livingston, J. D. *J. Appl. Phys.* **1959**, *30*, 120S.

Conclusions

The effectively unlimited reduction potential of the alkali metal anion makes the reduction of even the early transition elements and, as we have demonstrated in this report, gadolinium, not only possible but rapid. Alkalide reduction is probably applicable to other lanthanide metals as well and may be a route to nanoscale compounds and alloys thereof. For application as magnetic refrigerants, ferromagnetically interacting superparamagnetic gadolinium nanoparticles may be advantageous. Although the materials we report here are not in large part superferromagnetic, we do see some evidence of ferromagnetic coupling in some samples. This indicates that optimization/alteration of material processing parameters may be effective in increasing the interactions. Surface composition, crystallinity, or morphology can all have dramatic effects on the magnetic behavior of nanomaterials. It should be possible to increase the intra- and interparticle ferromagnetic coupling though control of these and other factors by postsynthesis processing and "tune" the behavior to achieve a highly effective magnetic refrigerant.

Acknowledgment. This research has been supported by a grant (R-82813201-0) from the U.S. Environmental Protection Agency's (EPA) Science to Achieve Results (STAR) program and the National Science Foundations CAREER program (DMR-9876164). Although the research described in the article has been funded in part by the U.S EPA's STAR program, it has not been subjected to any EPA review and therefore does not necessarily reflect the views of the Agency, and no official endorsement should be inferred. The authors thank Dr. Robert Shull and Dr. Richard Fry of NIST for assistance with magnetic measurements and Farhad Shirmohammadi for assistance with literature review. We would also like to thank Dr. Robin Rufner and the George Washington University Center for Microscopy and Image Analysis for assistance with TEM imaging and William Rutowski for machine shop assistance.

JA0122703